ACS APPLIED MATERIALS & INTERFACES

Research Article

www.acsami.org

Thermoresponse Improvement of Poly(*N*-isopropylacrylamide) Hydrogels via Formation of Poly(sodium *p*-styrenesulfonate) Nanophases

Jingang Li, Houluo Cong, Lei Li, and Sixun Zheng*

Department of Polymer Science and Engineering and the State Key Laboratory of Metal Matrix Composites, Shanghai Jiao Tong University, Shanghai 200240, People's Republic of China

ABSTRACT: The block copolymer networks composed of poly(*N*-isopropylacrylamide) (PNIPAM) and poly(sodium *p*-styrenesulfonate) were synthesized via sequential reversible addition−fragmentation chain transfer (RAFT) polymerization with α,ω-didithiobenzoate-terminated poly(sodium *p*-styrenesulfonate) (PSSNa) as the macromolecular chain transfer agent. It was found that the block copolymer networks were microphase-separated as evidenced by means of transmission electron microscopy (TEM) and small-angle X-ray scattering (SAXS). In the block copolymer networks, spherical or cylindrical PSSNa microdomains were finely dispersed into continuous PNIPAM matrixes. In comparison with unmodified PNIPAM hydrogel, the nanostructured hydrogels displayed improved thermoresponsive properties. In addition, the swelling ratios of the PSSNa-modified PNIPAM hydrogels were significantly higher than that of plain PNIPAM hydrogel. The improvement of thermoresponse was attributable to the formation of the PSSNa nanophases, which promoted the transportation of water molecules in the cross-linked networks.

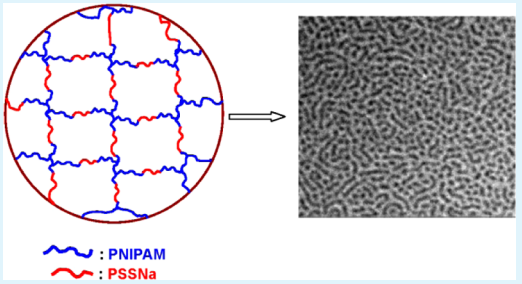

KEYWORDS: *PNIPAM, hydrogels, block copolymer, fast thermoresponsive properties*

INTRODUCTION

Polymeric hydrogels are a class of important soft matters and have been widely used as superabsorbent materials and for separation process and controlled drug delivery.[1−7] Thermoresponsive hydrogels have attracted considerable interest because they can vary in shape or volume in response to environmental temperature. Because of high water content and biocompatibility, the stimuli-responsive hydrogels are the materials of choice in a variety of biomedical applications.[4−7] It is well-known that poly(*N*-isopropylacrylamide) (PNIPAM) hydrogels can display a volume phase transition (VPT) while temperature is changed.[1,2,8,9] The VPT behavior results from the lower critical solution temperature (LCST) behavior of linear PNIPAM in aqueous solutions.[10−14] However, the reswelling and deswelling of unmodified PNIPAM hydrogels are inherently slow, and thus their direct application is greatly limited. It has been realized that the slow reswelling and deswelling behavior results from the formation of a dense and hydrophobic layer at the surface of the hydrogels with the occurrence of volume phase transition. The collective transportation of water in response to environmental temperature change would be retarded by the dense and hydrophobic layer.[15−18] To achieve the successful application, the measure must be taken to improve the thermoresponse of the hydrogels. One basic strategy is to interrupt the continuity of the dense and hydrophobic layer at the surface of hydrogels.[19−33] For instance, the deswelling and reswelling properties can be improved by preparing porous hydrogels.[19−21] Introducing the porosity is favorable to the contact of PNIPAM with water by increasing the interfaces between PNIPAM and water in the hydrogels. Nonetheless, the mechanical strength of the porous hydrogels could be significantly decreased. Recently, it has been realized that the thermoresponsive rate of PNIPAM hydrogels can be enhanced by incorporating hydrophilic components.[20,22,28,34−39] The hydrophilic components can be introduced into PNIPAM hydrogels in either a physical or a chemical way. For instance, several water-soluble polymers such as poly(*N*-vinylpyrrolidone) and poly(ethylene oxide), have been utilized as the modifiers to improve the thermoresponsive properties.[20,28,34−37] It is realized that the incorporation of the hydrophilic components facilitates the transportation of water in the cross-linked networks.[20,22,28,34−39] Nonetheless, the cause of the thermoresponsive improvement for the modified hydrogels has not been well elucidated. In addition, Okano et al.[22,38,39] reported that the PNIPAM hydrogels having comb-like architecture can display fast thermoresponsive properties. In the comb-like networks, there are some dangling PNIPAM chains grafted on the networks. It is believed that the high mobility of these dangling PNIPAM chains endows the PNIPAM hydrogels with improved thermoresponsive behavior.

Polyelectrolytes are polymers bearing ionizable groups; they can be ionized in water, keeping charges in the main chains of the polymer and leaving counterions in the whole solution. Because of electrostatic interactions between the charges of the

Received: May 21, 2014
Accepted: July 7, 2014
Published: July 18, 2014

   dx.doi.org/10.1021/am503148v | *ACS Appl. Mater. Interfaces* 2014, 6, 13677−13687

polymer backbone, the polyelectrolyte chains in aqueous solutions can display rich behavior quite different from that of uncharged polymers.[40,41] It is of interest to explore the utilization of highly hydrophilic polyelectrolyte to improve the thermoresponse of polymeric hydrogels.[42−46] In the past years, the modification of PNIPAM hydrogels by polyelectrolyte has been extensively reported by many investigators.[47−57] In previous reports, poly(methacrylic acid) (PMAA) and poly(acrylic acid) (PAA) have often been employed to improve the thermoresponse of PNIPAM hydrogels.[47−60] These weak polyelectrolytes are generally introduced into PNIPAM hydrogels with two approaches: (i) the random copolymerization of NIPAM with MAA (or/and AA)[47−54] and (ii) the formation of the interpenetrating polymer networks (IPNs).[55−60] In the random copolymerization approach, the electrolyte structural units were randomly distributed along the PNIPAM chains. It has been found that loading a considerable amount of MAA (or/and AA) could cause reduction and even elimination of the thermoresponse of the hydrogels.[61,64] For the IPNs of PNIPAM with polyelectrolyte, linear PMAA (or/and PAA) chains were interpenetrated into PNIPAM networks. Because of the architecture of semi-IPNs, the loss of the linear modifiers is inevitable in the process of swelling, deswelling, and reswelling. By comparison, the modification of PNIPAM hydrogels with strong polyelectrolytes remained largely unexplored.[63−67] In limited reports, the random copolymerization of NIPAM with strong electrolyte monomers such as sodium acrylate[65] and 2-acrylamido-2-methylpropanesulfonate[66] has been carried out to modify PNIPAM hydrogels. In comparison with the control hydrogel, the modified hydrogels exhibited increased swelling ratios and enhanced VPT temperatures.

In this work, we explored to improve the thermoresponse of PNIPAM hydrogels by using poly(sodium *p*-styrenesulfonate) (PSSNa), a strong polyelectrolyte (i.e., a permanently water-soluble polymer); PSSNa was incorporated into PNIPAM networks as the blocky subchains. To the best of our knowledge, there has been no previous report on the modification of PNIPAM hydrogels with polyelectrolyte via the formation of block copolymer networks. To achieve this, a sequential reversible addition−fragmentation chain transfer (RAFT) polymerization approach was employed to access the blocked PNIPAM networks. The morphologies of block copolymer networks were studied by means of transmission electron microscopy (TEM) and small-angle X-ray scattering (SAXS). The thermoresponsive properties of the hydrogels were examined in terms of swelling, deswelling, and reswelling tests. The improved thermoresponsive behavior was addressed on the basis of the formation of PSSNa nanophases in the PNIPAM networks.

EXPERIMENTAL SECTION

Materials. Sodium *p*-styrenesulfonate (SSNa) was of chemically pure grade, supplied by Shanghai Reagent Co. China. Before use, it was recrystallized from the mixture of water with methanol (20/80 vol). *N*-Isopropylacrylamide (NIPAM) was synthesized in this lab.[34] The initiator and cross-linker used in this work are 2,2-azobisisobutylnitrile (AIBN) and *N*,*N*′-methylenebis(acrylamide) (BIS), respectively; they were purchased from Shanghai Reagent Co., China. Prior to use, the initiator was recrystallized from alcohol twice. The chain transfer agent was 1,4-bis(thiobenzoylthiomethyl)-benzene; it was synthesized by following the method reported by Patton et al.[68] The organic solvents such as 1,4-dioxane, tetrahydrofuran (THF), and dimethyl sulfoxide (DMSO) were purchased from Shanghai Reagent Co, China. Before use, DMSO was distilled over anhydrous magnesium sulfate, and THF was refluxed over sodium and then distilled.

Synthesis of PSSNa-CTA. To a flask were charged SSNa (2.00 g, 9.709 mmol), 1,4-bis(thiobenzoylthiomethyl) benzene (0.092 g, 0.224 mmol), AIBN (0.006 g, 0.037 mmol), and DMSO (4.0 mL) with vigorous stirring. By the use of a Schlenk line, the flask was degassed via three freeze−evacuate−thaw cycles. The polymerization was allowed to perform at 65 °C for 12 h. After that, the polymerized product was dialyzed with water for 4 days to remove the unreacted monomer. The water was eliminated via rotary evaporation. The macromolecular chain transfer agent (denoted PSSNa-CTA) (1.60 g) was obtained with the yield of 76.5% after drying in vacuo at 35 °C for 24 h. By means of gel permeation chromatography, the molecular weight of PSSNa-CTA was measured to be M_n = 11 400 with M_w/M_n = 1.53.

Preparation of PNIPAM Network. Typically, to a glass tube with the diameter of 10 mm were charged NIPAM (1.000 g), anhydrous 1,4-dioxane (1.5 mL), and BIS (13.7 mg) with vigorous stirring. This system was purged with highly pure nitrogen for 30 min, and then AIBN (2.0 mg) was added with vigorous stirring. The polymerization was carried out at 60 °C for 24 h. The gelled product was extracted with deionized water for 7 days and then extracted with THF for 24 h, respectively. The majority of the absorbed THF was evaporated at room temperature for 24 h; the gel was further dried in vacuo at 60 °C to remove the residual solvent to constant weight.

Synthesis of PNIPAM-*b*-PSSNa Copolymer Networks. Typically, to a glass tube were charged NIPAM (0.800 g, 7.080 mmol), PSSNa-CTA (0.200 g, 0.029 mmol), BIS (0.011 g, 0.071 mmol), deionized water (1.0 mL), and 1,4-dioxane (0.8 mL) with vigorous stirring; AIBN (0.001 g, 0.006 mmol) was added. By using the Schlenk line, the system was degassed via three freeze−evacuate−thaw cycles. The polymerization was performed at 65 °C for at least 72 h. Cooled to room temperature, the gel was extracted with water for 7 days and with THF for 3 days. The majority of the absorbed THF was evaporated at 25 °C, and the residual solvent was eliminated under vacuum at 50 °C for 7 days. The gel was weighed to estimate the monomer conversion.

Measurements and Characterization. *Nuclear Magnetic Resonance (NMR) Spectroscopy.* The NMR measurements were conducted on a Varian Mercury Plus 400 MHz spectrometer at 25 °C. Deuterium chloroform (or water) was used as the solvent to dissolve the samples. The spectra were obtained with tetramethylsilane (TMS) as an external reference.

Gel Permeation Chromatography (GPC). The measurements of molecular weights were performed on a Perkin Elmer series 200 system equipped with 10 μm PL gel 300 × 7.5 mm mixed-B and mixed-C columns and with a refractive index (RI) detector. The aqueous solution of sodium nitrate ($NaNO_3$) (0.05 M) was used as the eluent at a flow rate of 0.6 mL/min. The measurement was performed at 40 °C; the molecular weights were expressed relative to poly(ethylene oxide) standards.

Small-Angle X-ray Scattering (SAXS). All of the scattering measurements were carried out in a SAXS station (BL16B1) of Shanghai Synchrotron Radiation Facility (SSRF), China. In this facility, a third generation of synchrotron radiation light source was utilized, and the X-ray with the wavelength of λ = 1.24 Å was rendered. In all of the measurements, 2-D diffraction patterns were recorded with an image intensified CCD detector. The intensity profiles were output as the plots of scattering intensity (I) versus scattering vector (q). To observe the microphase-separated morphologies, the dried gels were directly subjected to the SAXS measurements. To investigate the morphological evolution of the gels with swelling time, the gels were placed into small aluminum bags containing deionized water at 25 °C. The bags were subjected to SAXS measurements to in situ obtain the SAXS patterns with swelling time. Scattering profiles were recorded every 5 min until scattering phenomenon was no longer displayed.

Transmission Electron Microscopy (TEM). The morphological observation was conducted on a JEOL JEM-2010 transmission electron microscope at an acceleration voltage of 120 kV. The fully dried gels were ground into powder, which was then mixed with

Scheme 1. Synthesis of PSSNa-CTA and PNIPAM-*b*-PSSNa Copolymer Network

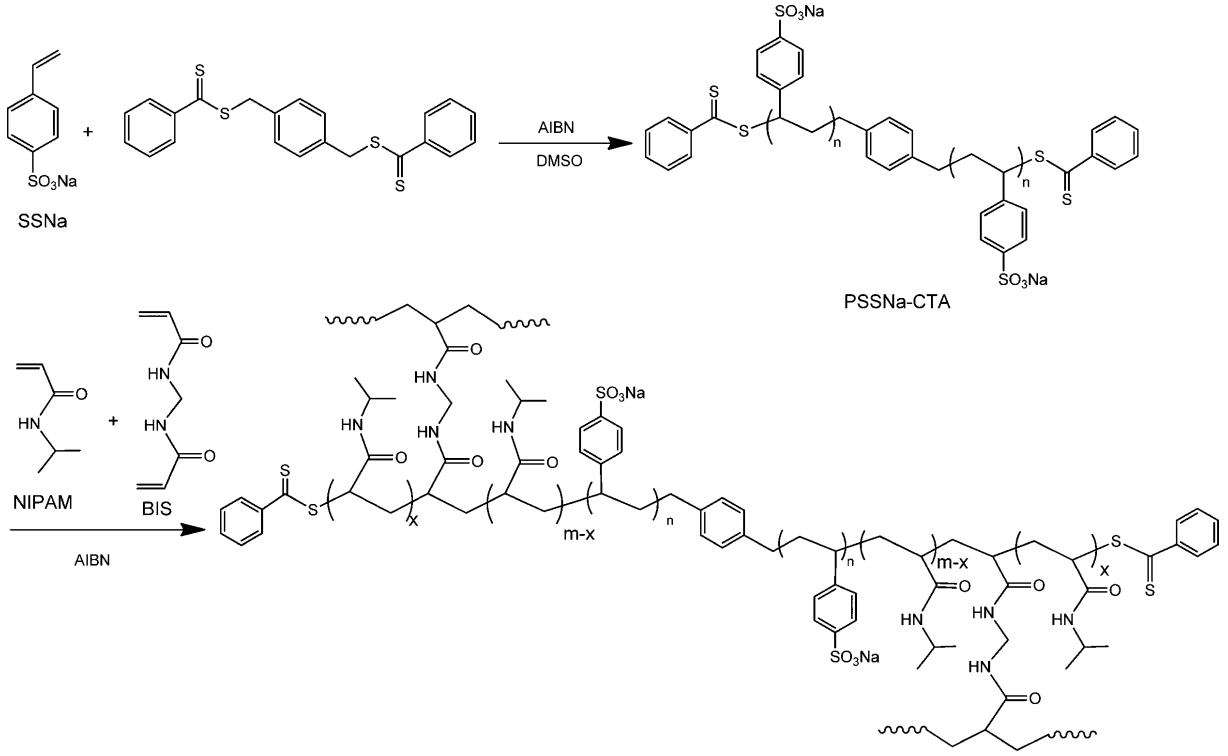

ethanol. The mixtures were dropped into 200 mesh copper grids. Before the measurement, ethanol was immediately removed in vacuo at room temperature.

Micro-Differential Scanning Calorimetry (Micro-DSC). The calorimetry was performed with a SETARAM Micro-DSC III differential scanning calorimeter. Before measurements, the fully swollen hydrogels (ca. 20 mg) were first held at 18 °C for 15 min. Thereafter, the samples were heated from room temperature to 60 °C at the rate of 1.0 °C/min in a nitrogen atmosphere. The VPT temperature was taken as the minimum of exothermic peak.

Swelling, Deswelling, and Reswelling Tests. The dried gels were sliced into discs with identical diameter of 10 mm and thickness of 4 mm. For the measurement of swelling ratios, the dried gels were fully swollen in distilled water at 24 °C for 72 h. After the water on the surface of the hydrogels was wiped off with moistened filter paper, swelling ratios were gravimetrically determined. The swelling ratios of the gels at various temperatures were recorded. Before the measurements, the specimens were held in distilled water at every particular temperature for 24 h. Swelling ratio (SR) is calculated according to the following equation:

$$\mathrm{SR} = W_s/W_d \quad (1)$$

where W_s is the weight of water absorbed in the hydrogel gel at a particular temperature, and W_d is the weight of the dried gel.

To investigate the deswelling behavior, all of the dried gels were first swelled in distilled water at 25 °C for 24 h. Thereafter, the swelled hydrogels were maintained in water at 48 °C for deswelling. After the water on the surface was wiped, the weights of the deswelled gels were measured at regular time intervals. According to the following equation, water retention (WR) is calculated:

$$\mathrm{WR} = (W_t - W_d)/W_s \times 100\% \quad (2)$$

where W_t is the weight of the deswelled gel; the other symbols are the same as in eq 1.

In the reswelling experiment, the swelled hydrogels were first dehydrated in a water bath at 48 °C for 24 h. Thereafter, the deswelled gels were immersed into water of 24 °C for reswelling. The weights of the reswelled gels at regular time intervals were gravimetrically measured. Water uptake (WU) is calculated according to the following equation:

$$\mathrm{WU} = (W_t - W_d)/W_s \times 100\% \quad (3)$$

where W_t is the weight of the reswelled gels at regular time intervals; the other symbols are the same as defined above.

Cycles of Swelling and Shrinking. To examine the thermoresponsive switching behavior of the hydrogels, four swelling−shrinking cycles were performed. In each cycle, the swelling ratios were first measured at 25 °C, and then the temperature was enhanced to 48 °C at the heating rate of 2 °C/min. Before the swelling ratios were determined, the hydrogels were stabilized at 25 or 48 °C for 2 h.

RESULTS AND DISCUSSION

Synthesis of PNIPAM-*b*-PSSNa Copolymer Networks. The route of synthesis for poly(*N*-isopropylacrylamide)-*block*-poly(sodium *p*-styrenesulfonate) (denoted PNIPAM-*b*-PSSNa) copolymer networks was depicted in Scheme 1. First, an α,ω-didithiobenzoate-terminated PSSNa was synthesized via the RAFT polymerization of SSNa with 1,4-bis-(thiobenzoylthiomethyl)benzene as the chain transfer agent (CTA). Second, the above α,ω-didithiobenzoate-terminated PSSNa was employed as a macromolecular CTA (denoted PSSNa-CTA), and the RAFT polymerization of NIPAM was carried out to obtain the PNIPAM-*b*-PSSNa block copolymer networks with BIS as the cross-linker. The ^{1}H NMR spectra of 1,4-bis(thiobenzoylthiomethyl)benzene and PSSNa-CTA are shown in Figure 1. For the former, the signal of resonance at 4.6 ppm was assignable to the protons of methylene groups, whereas those at 7.3−8.0 ppm were assigned to the protons of aromatic rings. The ratio of the integral intensity of the methylene protons to those of the aromatic ring protons was measured to be ca. 1:3.5, which was identical to the value calculated according to the structural formula of 1,4-bis-(thiobenzoylthiomethyl)benzene, indicating that the chain

dx.doi.org/10.1021/am503148v | ACS Appl. Mater. Interfaces 2014, 6, 13677−13687

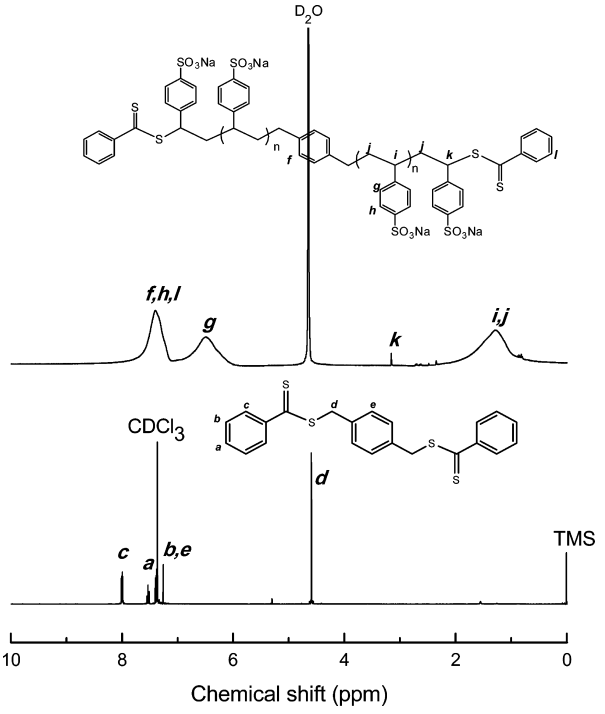

Figure 1. ^{1}H NMR spectra of 1,4-bis(thiobenzoylthiomethyl)benzene in $CDCl_3$ and PSSNa-CTA in D_2O.

transfer agent was successfully obtained. For PSSNa-CTA, the new signals of resonance were detected at 1.28 and 3.14 ppm; they were assignable to the protons of methine and methylene groups in the main chain of PSSNa, respectively. In addition, the resonance of the methine protons of benzene ring was detected between 6.00 and 8.00 ppm. This polymer was subjected to GPC, and the molecular weight was measured to be M_n = 11 400 with M_w/M_n = 1.53. The results of ^{1}H NMR and GPC indicate that the PSSNa-CTA was successfully obtained. The PSSNa-CTA was employed to mediate the radical polymerization of NIPAM monomer to obtain the PNIPAM-*b*-PSSNa block copolymer networks via RAFT, while BIS was used as the cross-linker. To remove unreacted NIPAM monomer, the cross-linked products were extracted with distilled water for 1 week, and then the absorbed water was eliminated via extraction with THF for 3 days. The gels were further dried in vacuo to constant weight. Assuming that PSSNa was fully incorporated into the cross-linked networks, the compositions of the block copolymer networks can be estimated in terms of the yields of the gels. The conversion of the monomer and the compositions of copolymer networks are summarized in Table 1. Notably, the conversions of NIPAM monomer were as high as 80% under the present condition. The results of polymerization suggest that PNIPAM-*b*-PSSNa block copolymer networks were successfully obtained.

Table 1. Results of Polymerization for the Preparation of PNIPAM-*b*-PSSNa Networks

samples	feed of PSSNa (wt %)	conversion of NIPAM (mol %)	PSSNa (wt %)
PNIPAM-*b*-PSSNa5	5	83.3	5.9
PNIPAM-*b*-PSSNa10	10	79.1	12.3
PNIPAM-*b*-PSSNa15	15	78.8	18.3
PNIPAM-*b*-PSSNa20	20	76.0	24.8

Nanostructures of PNIPAM-*b*-PSSNa Networks. All of the dried PNIPAM-*b*-PSSNa gels were transparent and homogeneous, implying that no macroscopic phase separation occurred. Nonetheless, the clarity did not exclude the possible microphase separation in the dried gels. To examine the morphology, the PNIPAM-*b*-PSSNa dried gels were subjected to transmission electron microscopy (TEM), and the TEM micrographs are shown in Figure 2. Notably, the microphase-separated morphologies were displayed. In terms of the

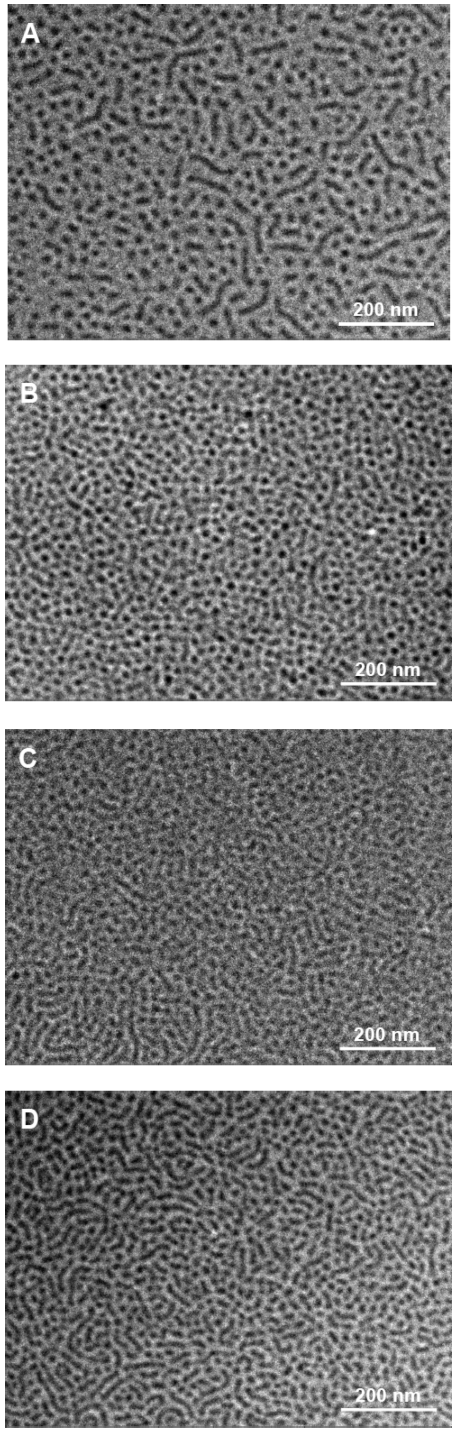

Figure 2. TEM micrographs of (A) PNIPAM-*b*-PSSNa5, (B) PNIPAM-*b*-PSSNa10, (C) PNIPAM-*b*-PSSNa15, and (D) PNIPAM-*b*-PSSNa20.

difference in electron density between PNIPAM and PSSNa, it is judged that the dark microdomains are attributable to PSSNa, whereas the light region is from PNIPAM. For PNIPAM-*b*-PSSNa5, the spherical and cylindrical PSSNa microdomains with size of 10−20 nm in diameter were dispersed in the continuous PNIPAM matrix. As the content of PSSNa increased, the percentage of cylindrical PSSNa microdomains significantly increased. Meanwhile, the PSSNa cylindrical microdomains become slightly thin (see Figure 2B−D).

The microphase-separated morphologies were further confirmed by SAXS. The SAXS profiles of the PNIPAM-*b*-PSSNa networks are presented in Figure 3. Notably, the intense

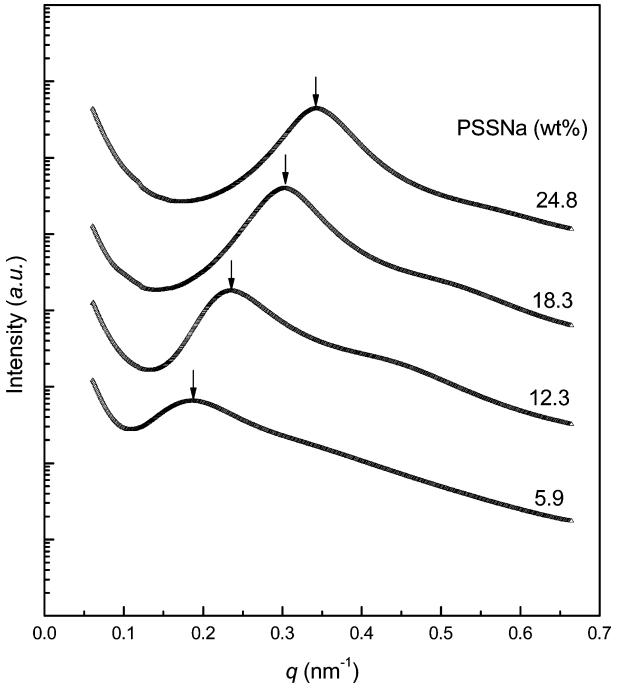

Figure 3. SAXS profiles of PNIPAM-*b*-PSSNa copolymer networks.

scattering peaks were displayed. The scattering phenomenon indicates that all of the dried PNIPAM-*b*-PSSNa gels were indeed microphase-separated. This result was in good agreement with the TEM result. For PNIPAM-*b*-PSSNa5, the scattering peak appeared at ca. $q = 0.19$ nm^{-1}. As the content of PSSNa was increased, the scattering peaks were shifted to the positions with the higher q values. According to the positions (q) of the primary scattering peaks, the average distances between adjacent PSSNa microdomains were calculated to be 33.8, 26.9, 20.9, and 18.4 nm for PNIPAM-*b*-PSSNa5, PNIPAM-*b*-PSSNa10, PNIPAM-*b*-PSSNa15, and PNIPAM-*b*-PSSNa20 networks, respectively. The formation of the PSSNa nanophases was very important for the thermoresponse improvement of the PNIPAM hydrogels.

Volume Phase Transition Behavior of PNIPAM-*b*-PSSNa Hydrogels. The above PNIPAM-*b*-PSSNa dried gels were subjected to swelling tests with water. It was seen that these block copolymer networks were significantly swelled without dissolving; that is, the hydrogels were obtained. These hydrogels were transparent and homogeneous at low temperature (e.g., <30 °C). Upon heating to elevated temperatures (e.g., >40 °C), they became cloudy and shrank, implying that volume phase transition (VPT) behavior occurred (see Figure 4). It should be pointed out that the orange color of the dried gel (Figure 4A) was from the fragments of the chain transfer agent, that is, dithiobenzoate moieties.

The VPT temperatures of the PNIPAM-*b*-PSSNa hydrogels were measured by means of micro-differential scanning calorimetry (Micro-DSC) as shown in Figure 5. In the heating DSC scans, the PNIPAM-*b*-PSSNa hydrogels exhibited single exothermic peaks as the plain PNIPAM hydrogel. The exothermic peaks were attributable to the VPT behavior of the thermoresponsive hydrogels. These exothermic peaks were asymmetrical with steep leading sides before the minima. For the plain PNIPAM hydrogel, the temperature of VPT was measured to be ca. 33.3 °C. As PSSNa was incorporated into the hydrogel, the VPT temperatures were significantly shifted to higher temperatures. Notably, the VPT temperature of PNIPAM-*b*-PSSNa15 hydrogel was measured to be 37.3 °C, and this value was quite close to the temperature of the human body. The increase in VPT temperatures resulted from the incorporation of PSSNa blocks in the cross-linked networks. The inclusion of the highly hydrophilic PSSNa enhanced the affinity of the cross-linked networks with water, and thus the VPT occurred at higher temperatures. Also shown in Figure 5 (see the inset) is the plot of the exothermic enthalpy (ΔH_{VPT}) versus the mass percentage of PSSNa. It is proposed that the VPT enthalpy (denoted ΔH_{VPT}) is proportional to the quantity of the PNIPAM segments that underwent the volume phase transition. If the VPT of PNIPAM chains were not influenced by PSSNa blocks, a straight line of ΔH_{VPT} against the mass fraction of PNIPAM should be drawn. In the present case, nonetheless, the experimental ΔH_{VPT} values were much lower than those theoretically estimated according to the additive. The bigger was the deviation, the higher was the content of

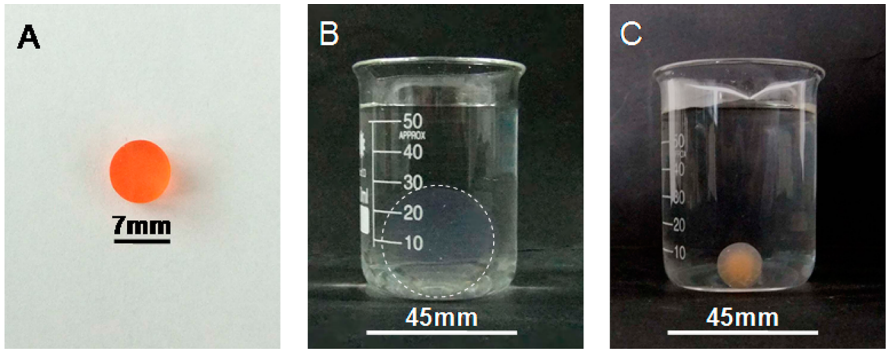

Figure 4. Photographs of PNIPAM-*b*-PSSNa10 copolymer network: (A) the dried gel, (B) the gel swelled at 24 °C for 24 h, and (C) the hydrogel deswelled at 48 °C for 24 h.

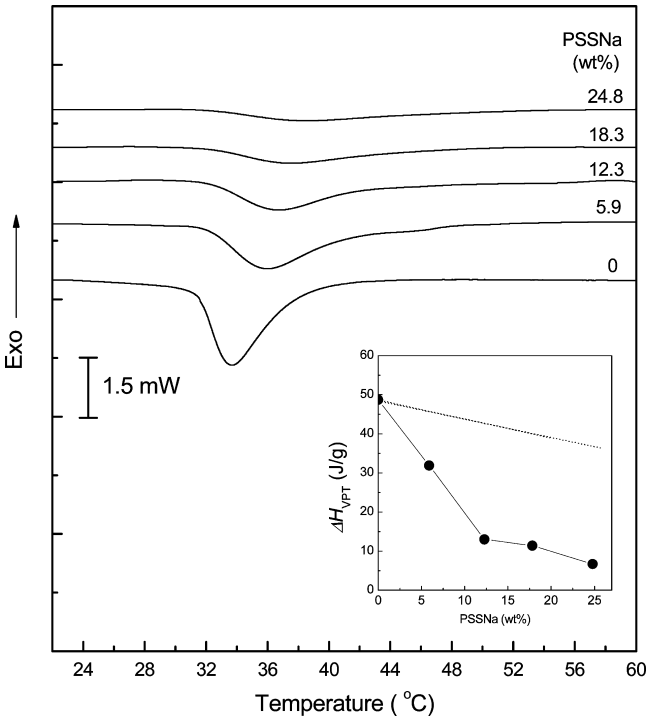

Figure 5. Micro-DSC profiles of the control PNIPAM and PNIPAM-*b*-PSSNa hydrogels.

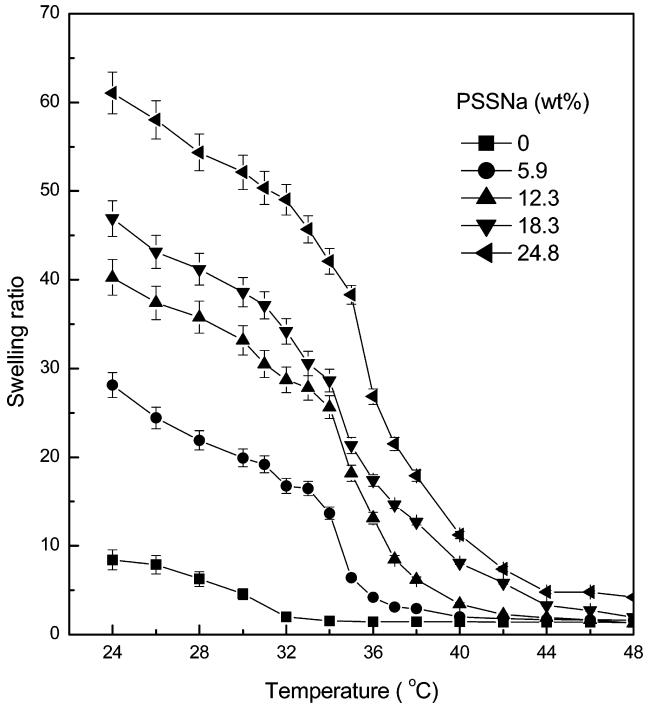

Figure 6. Swelling ratios of the control PNIPAM and PNIPAM-*b*-PSSNa hydrogels at various temperatures.

PSSNa. This result implies that a part of the PNIPAM segments failed to undergo the coil-to-globule transition in the swelled networks. It is plausible to propose that those PNIPAM segments intimately bonded to PSSNa blocks could be restricted by the PSSNa blocks and thus failed to undergo the coil-to-globule transition. These PNIPAM segments could still remain hydrophilic even while the hydrogels were heated to above the VPT temperature.

Swelling, Deswelling, and Reswelling Properties. The thermoresponsive properties of the PSSNa-modified PNIPAM hydrogels were investigated in terms of swelling, deswelling, and reswelling tests. Figure 6 presented the plots of swelling ratios versus temperature for plain PNIPAM and the modified hydrogels. The inverse sigmoid curves were exhibited for all of these hydrogels, characteristic of the VPT behavior of the thermoresposive hydrogels. From these curves, the VPT temperatures of the hydrogels can be estimated. Notably, the swelling curves of all of the modifed hydrogels were on the right-hand side of the control hydrogel, indicating that the VPT temperatures of the hydrogels were enhanced with the incorporation of PSSNa component. It is seen that the VPT temperatures increased as the PSSNa contents increased. This result was in good agreement with that of Micro-DSC measurements. At 24 °C, the swelling ratio of the control PNIPAM hydrogel was measured to be ca. 8.60. At the same temperature, the swelling ratios of PNIPAM-*b*-PSSNa5, PNIPAM-*b*-PSSNa10, PNIPAM-*b*-PSSNa15, and PNIPAM-*b*-PSSNa20 hydrogels were 28.1, 40.2, 46.9, and 61.3, respectively; they all were much higher than the control PNIPAM hydrogel. The swelling ratios increased as the content of PSSNa increased. For the control hydrogel, the swelling ratio of the control PNIPAM hydrogel was reduced from 8.60 at 24 °C to 1.48 at 48 °C; that is, 82.8 wt % of the absorbed water was released. Under identical conditions, nonetheless, 95.5%, 94.7%, 95.1%, and 93.1% of absorbed water were released for PNIPAM-*b*-PSSNa5, PNIPAM-*b*-PSSNa10, PNIPAM-*b*-PSSNa15, and PNIPAM-*b*-PSSNa20 hydrogels, respectively.

In the deswelling tests, the fully swollen hydrogels were first held at 48 °C to dehydrate, and then the swelling ratios of the hydrogels were determined at regular time intervals. The water retention of the gels was plotted as functions of deswelling time as shown in Figure 7. Notably, the water uptakes of all of the PSSNa-modified hydrogels were much lower than that of the

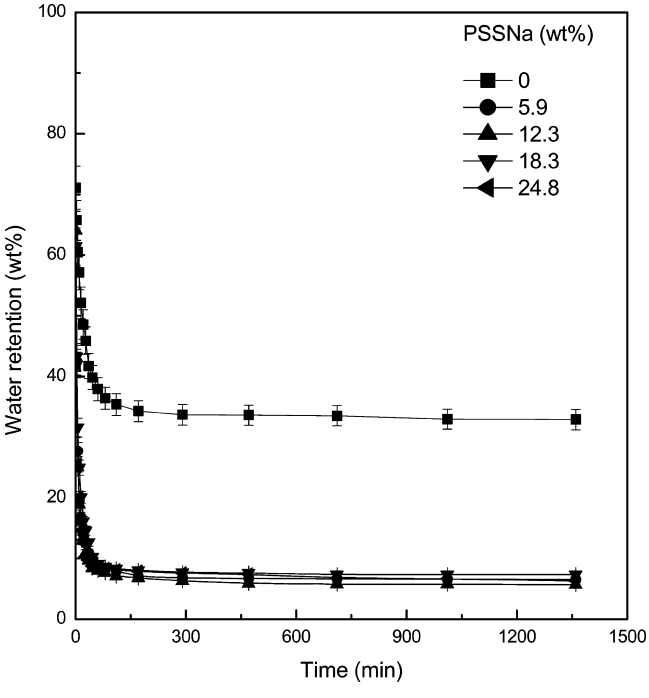

Figure 7. Plots of water uptakes as functions of deswelling time for the control PNIPAM and PNIPAM-*b*-PSSNa hydrogels.

dx.doi.org/10.1021/am503148v | *ACS Appl. Mater. Interfaces* 2014, 6, 13677−13687

plain PNIPAM hydrogel. The deswelling experiments showed that within the same time, all of the PNIPAM-*b*-PSSNa hydrogels released the absorbed water much more than the control PNIPAM hydrogel. For the control PNIPAM hydrogel, the water retention was measured to be 32% after it was deswelled at 48 °C for 1360 min. In contrast, the water retentions were as low as 7.2% for all of the modified hydrogels. Furthermore, the PSSNa-modified hydrogels attained the stable water retentions much faster than the control hydrogel. For the control PNIPAM hydrogel, it took ca. 37 min to reach its stable water retention of ca. 41.0%. Within the identical time, however, the water retentions of the PNIPAM-*b*-PSSNa hydrogels were as low as 8.6 wt %. In terms of the above results, it is judged that the deswelling of the PNIPAM-*b*-PSSNa hydrogels was much faster than that of the control PNIPAM hydrogel.

To investigate the reswelling hehavior of all of the dehydrated gels, the swelled hydrogels were first dehydrated in distilled water at 48 °C for 24 h. Thereafter, the deswelled gels were immersed into water of 24 °C to allow reswelling. Shown in Figure 8 are the plots of water uptake versus

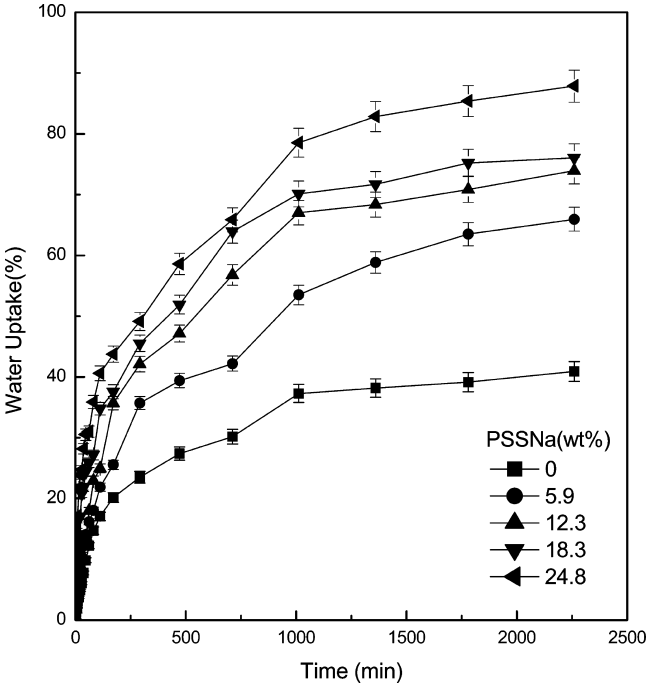

Figure 8. Plots of water uptake as functions of reswelling time for the control PNIPAM and the PNIPAM-*b*-PSSNa hydrogels.

reswelling time. With the same reswelling time, the PSSNa-modified hydrogels had water uptakes much higher than that of the plain hydrogel. This result indicates that the PNIPAM-*b*-PSSNa hydrogels deswelled much faster than the plain PNIPAM hydrogel. As the content of PSSNa increased, the water uptakes of the PNIPAM-*b*-PSSNa hydrogels increased. For PNIPAM-*b*-PSSNa5, PNIPAM-*b*-PSSNa10, PNIPAM-*b*-PSSNa15, and PNIPAM-*b*-PSSNa20 hydrogels, the water uptakes were measured to be 42.2, 56.8, 63.1, and 66.3 after they were reswelled for 600 min, which were much larger than that of the control PNIPAM hydrogel (i.e., 30.2%). This experiment shows that the reswelling rates of the PNIPAM-*b*-PSSNa were much higher than that of the plain PNIPAM hydrogel.

To examine the thermoresponsive switching behavior of the hydrogels, the modified hydrogels were subjected to circular 2 hour-swelling−shrinking experiments in step changes of temperature between 25 and 48 °C. Shown in Figure 9 are

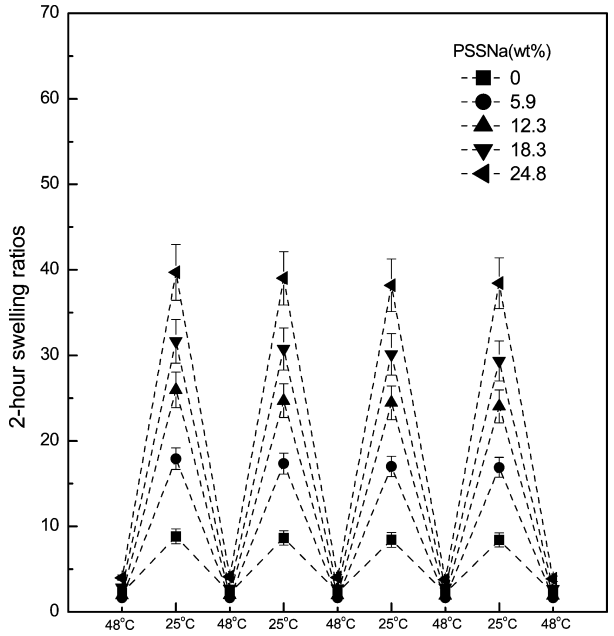

Figure 9. Four cycles of swelling−deswelling switching experiments of the hydrogels between 25 and 48 °C for the control PNIPAM and the PNIPAM-*b*-PSSNa hydrogels.

the plots of swelling ratios versus the temperature of 25 or 48 °C for the control PNIPAM and PNIPAM-*b*-PSSNa hydrogels. As compared to the control hydrogel, there were only slight decreases in swelling ratios after the copolymer hydrogels experienced four cycles of swelling−shrinking experiments, suggesting that the modified hydrogels exhibited quite good swelling−shrinking switch performance.

Interpretation of Hydrogel Behavior. *Swelling Ratios.* The PNIPAM-*b*-PSSNa hydrogels possessed swelling ratios much higher than that of the control PNIPAM hydrogel; the swelling ratios increased with increasing fraction of PSSNa. The increased swelling ratios are attributable to (i) the incorporation of PSSNa component and (ii) the lowered cross-linking densities of the copolymer networks. It is known that the hydration degree of the polyelectrolyte (i.e., PSSNa) was much higher than that of PNIPAM. Therefore, the incorporation of PSSNa in place of PNIPAM would cause the increase in the hydration degree of the cross-linked networks. In addition, the increased swelling ratios were associated with the decrease in cross-linking densities of the PNIPAM-*b*-PSSNa networks in comparison with the control PNIPAM network. In the preparation of the PNIPAM-*b*-PSSNa copolymer networks, the molar ratio of the cross-linker (viz., BIS) to NIPAM monomer was controlled to be a constant; that is, the quantity of BIS was 1 mol % of NIPAM monomer. Therefore, the overall cross-linking densities of the PNIPAM-*b*-PSSNa networks were lower than that of the control PNIPAM network. In other words, the average molecular weights between the adjacent cross-linking sites for the PNIPAM-*b*-PSSNa networks were higher than those of the control PNIPAM network. The cross-linking densities would decrease with increasing concentration of PSSNa. The decreased cross-linking densities resulted

in the decrease in swelling ratios of the modified hydrogels. It is proposed that the decreased cross-linking densities of the PNIPAM-*b*-PSSNa netowrks can be compensated by increasing the quantity of cross-linker (viz., BIS) while the cross-linked networks were prepared. To confirm this, we prepared the PNIPAM-*b*-PSSNa hydrogels by the use of various amounts of cross-linker. Shown in Figure 10 is the plot of swelling ratio of

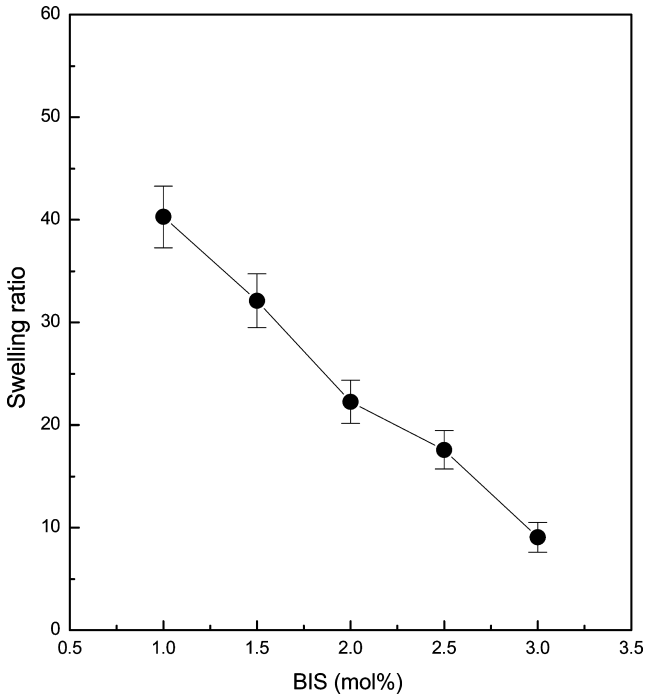

Figure 10. Swelling ratios of PNIPAM-*b*-PSSNa10 hydrogel at various molar fractions of BIS to NIPAM.

PNIPAM-*b*-PSSNa10 hydrogel as a function of the molar ratio of BIS to NIPAM. Notably, the swelling ratio decreased with increasing quantity of BIS.

Swelling (or Reswelling) Rate. The results of TEM and SAXS showed that the PNIPAM-*b*-PSSNa networks displayed the microphase-separated morphologies, in which spherical or cylindrical nanophases were finely dispersed into a continuous PNIPAM matrix. The PSSNa nanophases could play a significant role in accelerating the swelling (or reswelling) and deswelling of the hydrogels. In the swelling (or reswelling) experiments, the hydrophilic PSSNa microdomains can be rapidly hydrated. As a result, there was the very huge interface between PNIPAM matrix and hydrated PSSNa nanophases in the cross-linked networks. Therefore, the swelling (or reswelling) was significantly accelerated. The higher were the PSSNa concentrations in the networks, the faster was the swelling (or reswelling) of the gels. To confirm this speculation, we examined the morphological evolution of the gels as functions of swelling time with time-resolved SAXS. Representatively shown in Figure 11 are the SAXS profiles of PNIPAM-*b*-PSSNa15 gel at various swelling times at 25 °C. At t = 0 min, the dried gel displayed an intense scattering peak at q = 0.36 nm^{-1}, indicating that the dried gel was microphase-separated. Notably, the intensity of this scattering peak gradually decreased with increasing swelling time. While the gel was swollen for 95 min, the scattering peak became indiscernible. The decrease in scattering peak intensity suggests that the difference in electron density between PNIPAM matrix

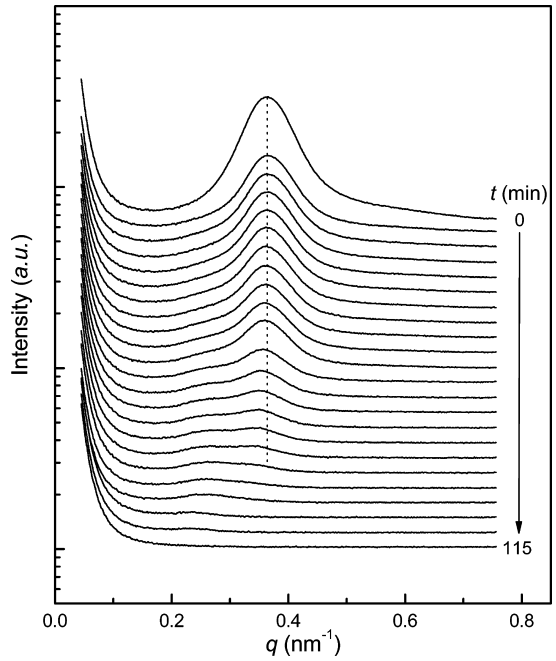

Figure 11. SAXS profiles of PNIPAM-*b*-PSSNa15 gel at various swelling times at 25 °C.

and PSSNa microdomains was increasingly decreased as both PNIPAM matrix and PSSNa microdomain were simultaneously hydrated. This judgment was also confirmed by the observation that the position of the scattering peak remained almost invariant at q = 0.36 nm^{-1}. It is proposed that two opposite factors influenced the positions of the scattering peaks. On the one hand, the scattering peak would be shifted to the position of higher q values with the hydration of the PSSNa microdomains because the average distance between adjacent PSSNa microdomains was shortened with the occurrence of the hydration of PSSNa microdomains. On the other hand, the average distance between adjacent PSSNa microdomains would be increased with the increase in the dimension of the gel due to the occurrence of swelling. With the occurrence of the swelling phenomenon, the volume of the gels increased, and the average distance between adjacent PSSNa microdomains would be increased. In the present case, however, the position of the scattering peak remained almost invariant in the swelling process. This observation implied that the effects of the above opposite factors on q values were almost counteracted. It should be pointed out that there could be some delay in swelling to reach the core of the gel in the SAXS measurement. Nonetheless, the SAXS results indeed indicate that both the swelling of PNIPAM matrix and the hydration of PSSNa microdomain were simultaneously performed. In other words, the PSSNa microdomains in the gels promoted the interfacial contact between PNIPAM matrix and water, and thus the swelling (or reswelling) was accelerated.

Deswelling Rate. The VPT behavior of the hydrogels stemmed from the coil-to-globule transition of PNIPAM chains in the swelled networks. As the environmental temperature was enhanced, the hydrated PNIPAM chains in the cross-linked networks gradually became dehydrated. For unmodified PNIPAM hydrogel, the dehydration occurred gradually from the surface to the interior of the hydrogel; that is, a dense hydrophobic layer was formed at the surface of hydrogel. This layer constituted a restriction of collective diffusion of water. As

a consequence, the deswelling process became slower.[15−18] For the PNIPAM-*b*-PSSNa hydrogels, nonetheless, the situation was quite different. In the deswelling process, the highly hydrophilic PSSNa microdomains in place of dehydrated PNIPAM layer interrupted the continuity of the dense and hydrophobic layer, which facilitated the transportation of water molecules from the interior to surfaces of the dehydrated gels. As a result, the accelerated deswelling for the PNIPAM-*b*-PSSNa hydrogels was exhibited; the deswelling rates were much higher than that of the plain PNIPAM. Meanwhile, the water uptakes of all of the PSSNa-modified hydrogels were much lower than that of the control PNIPAM gel.

CONCLUSION

The thermoresponsive improvement of PNIPAM hydrogels was carried out via the formation of polyelectrolyte nanophases. An α,ω-didithiobenzoate-terminated poly(sodium *p*-styrenesulfonate) was synthesized and used as a macromolecular chain transfer agent to obtain the PNIPAM-*b*-PSSNa block copolymer networks via RAFT polymerization approach with BIS as the cross-linker. Transmission electron microscopy and small-angle X-ray scattering showed that the block copolymer networks exhibited the microphase-separated morphologies, in which spherical or cylindrical PSSNa nanophases were dispersed into a continuous PNIPAM matrix. It was found that the PNIPAM-*b*-PSSNa hydrogels possessed swelling ratios significantly higher than the control PNIPAM hydrogel at room temperature. In comparison with the control PNIPAM hydrogel, the deswelling and reswelling of the modified hydrogels were in accelerated fashions. The rapid thermoresponse of the modified hydrogels was attributable to the formation of PSSNa nanophases in PNIPAM networks.

AUTHOR INFORMATION

Corresponding Author

*Tel.: 86-21-54743278. Fax: 86-21-54741297. E-mail: szheng@sjtu.edu.cn.

Notes

The authors declare no competing financial interest.

ACKNOWLEDGMENTS

We thank the Natural Science Foundation of China for financial support under project nos. 51133003 and 21274091. We also thank the Shanghai Synchrotron Radiation Facility for help in the SAXS measurements under project nos. 10sr0260 and 10sr0126.

REFERENCES

(1) Hirokawa, Y.; Tanaka, T. Volume Phase Transition in a Nonionic Gel. *J. Chem. Phys.* **1984**, *81*, 6379−6380.
(2) Matsuo, E. S.; Tanaka, T. Kinetics of Discontinuous Volume-Phase Transition of Gels. *J. Chem. Phys.* **1988**, *89*, 1695−1703.
(3) Suzuki, A.; Tanaka, T. Phase-Transition in Polymer Gels Induced by Visible-Light. *Nature* **1990**, *346*, 345−347.
(4) Kikuchi, A.; Okano, T. Intelligent Thermoresponsive Polymeric Stationary Phases for Aqueous Chromatography of Biological Compounds. *Prog. Polym. Sci.* **2002**, *27*, 1165−1193.
(5) Gil, E. S.; Hudson, S. M. Stimuli-Reponsive Polymers and Their Bioconjugates. *Prog. Polym. Sci.* **2004**, *29*, 1173.
(6) Hoare, T.; Pelton, R. Engineering Glucose Swelling Responses in Poly(N-isopropylacrylamide)-Based Microgels. *Macromolecules* **2007**, *40*, 670−678.
(7) Zhang, X.-Z.; Xu, X.-D.; Cheng, S.-X.; Zhuo, R.-X. Strategies to Improve the Response Rate of Thermosensitive PNIPAM Hydrogels. *Soft Matter* **2008**, *4*, 385−391.
(8) Zhu, P. W.; Napper, D. H. Experimental Observation of Coil-to-Globule Type Transitions at Interfaces. *J. Colloid Interface Sci.* **1994**, *164*, 489−494.
(9) Yin, X.; Hoffman, A. S.; Stayton, P. S. Poly(N-isopropylacrylamide-co-propylacrylic acid) Copolymers that Respond Sharply to Temperature and pH. *Biomacromolecules* **2006**, *7*, 1381−1385.
(10) Heskins, M.; Guillet, J. E.; James, E. Solution Properties of Poly(*N*-isopropylacrylamide). *J. Macromol. Sci., Chem.* **1968**, *A2*, 1441−1455.
(11) Kujawa, P.; Tanaka, F.; Winnik, F. M. Temperature-Dependent Properties of Telechelic Hydrophobically Modified Poly(N-isopropylacrylamides) in Water: Evidence from Light Scattering and Fluorescence Spectroscopy for the Formation of Stable Mesoglobules at Elevated Temperatures. *Macromolecules* **2006**, *39*, 3048−3055.
(12) Schild, H. G. Poly(*N*-isopropylacrylamide): Experiment, Theory and Application. *Prog. Polym. Sci.* **1992**, *17*, 163−249.
(13) Wu, C.; Zhou, S. Volume Phase Transition of Swollen Gels: Discontinuous or Continuous? *Macromolecules* **1997**, *30*, 574−576.
(14) Kujawa, P.; Winnik, F. M. Volumetric Studies of Aqueous Polymer Solutions Using Pressure Perturbation Calorimetry: A New Look at the Temperature-Induced Phase Transition of Poly(N-isopropylacrylamide) in Water and D_2O. *Macromolecules* **2001**, *34*, 4130−4135.
(15) Gutowska, A.; Bae, Y. H.; Feijen, J.; Kim, S. W. Heparin Release from Thermosensitive Hydrogels. *J. Controlled Release* **1992**, *22*, 95−104.
(16) Turner, K.; Zhu, P. W.; Napper, D. H. Coil-To-Globule Transitions Of Interfacial Copolymers In Better Than Theta-Solvents. *Colloid Polym. Sci.* **1996**, *274*, 622−627.
(17) Stenzel, M. H.; Davis, T. P. Star Polymer Synthesis Using Trithiocarbonate Functional-Cyclodextrin Cores (Reversible Addition−Fragmentation Chain-Transfer Polymerization). *J. Polym. Sci., Part A: Polym. Chem.* **2002**, *40*, 4498−4512.
(18) Wu, X. S.; Hoffman, A. S.; Yager, P. Synthesis and Characterization of Thermally Reversible Macroporous Poly(N-Lsopropylacrylamide) Hydrogels. *J. Polym. Sci., Part A: Polym. Chem.* **1992**, *30*, 2121−2129.
(19) Kato, N.; Sakai, Y.; Shibata, S. Wide-Range Control of Deswelling Time for Thermosensitive Poly(N-isopropylacrylamide) Gel Treated by Freeze-Drying. *Macromolecules* **2003**, *36*, 961−963.
(20) Zhang, X.-Z.; Yang, Y.-Y.; Chung, T.-S.; Ma, K.-X. Preparation and Characterization of Fast Response Macroporous Poly(N-isopropylacrylamide) Hydrogels. *Langmuir* **2001**, *17*, 6094−6099.
(21) Serizawa, T.; Wakita, K.; Akashi, M. Rapid Deswelling of Porous Poly(N-isopropylacrylamide) Hydrogels Prepared by Incorporation of Silica Particles. *Macromolecules* **2002**, *35*, 10−12.
(22) Yoshida, R.; Uchida, K.; Kaneko, Y.; Sakai, K.; Kikuchi, A.; Sakurai, Y.; Okano, T. Comb-Type Grafted Hydrogels with Rapid Deswelling Response to Temperature Changes. *Nature* **1995**, *374*, 240−242.
(23) Li, Y.; Tanaka, T. Kinetics of Swemng and Shrinking of Gels. *J. Chem. Phys.* **1990**, *92*, 1365−1371.
(24) Ju, H. K.; Kim, S. Y.; Lee, Y. M. pH/Temperature-Responsive Behaviors of Semi-IPN and Comb-type Graft Hydrogels Composed of Alginate and Poly(*N*-isopropylacrylamide). *Polymer* **2001**, *42*, 6851−6857.
(25) Annaka, M.; Matsuura, T.; Kasai, M.; Nakahira, T.; Hara, Y.; Okano, T. Preparation of Comb-Type N-Isopropylacrylamide Hydrogel Beads and Their Application for Size-Selective Separation Media. *Biomacromolecules* **2003**, *4*, 395−403.
(26) Guiseppi-Elie, A.; Sheppard, N. F.; Brahim, S.; Narinesingh, D. Enzyme Microgels in Packed-Bed Bioreactors with Downstream Amperometric Detection Using Microfabricated Interdigitated Microsensor Electrode Arrays. *Biotechnol. Bioeng.* **2001**, *75*, 475−484.
(27) Nykänen, A.; Nuopponen, M.; Laukkanen, A.; Hirvonen, S.-P.; Rytelä, M.; Turunen, O.; Tenhu, H.; Mezzenga, R.; Ikkala, O.;

Ruokolainen, J. Phase Behavior and Temperature-Responsive Molecular Filters Based on Self-Assembly of Polystyrene-block-poly(N-isopropylacrylamide)-block- polystyrene. *Macromolecules* **2007**, *40*, 5827−5834.
(28) Kaneko, Y.; Nakamura, S.; Sakai, K.; Aoyagi, T.; Kikuchi, A.; Sakurai, Y.; Okano, T. Rapid Deswelling Response of Poly(N-isopropylacrylamide) Hydrogels by the Formation of Water Release Channels Using Poly(ethylene oxide) Graft Chains. *Macromolecules* **1998**, *31*, 6099−6105.
(29) Hayashi, H.; Kono, K.; Takagishi, T. Temperature-Dependent Associating Property of Liposomes Modified with a Thermosensitive Polymer. *Bioconjugate Chem.* **1998**, *9*, 382−389.
(30) Zhang, X.-Z.; Zhuo, R.-X. Dynamic Properties of Temperature-Sensitive Poly(N-isopropylacrylamide) Gel Cross-Linked through Siloxane Linkage. *Langmuir* **2001**, *17*, 12−16.
(31) Haraguchi, K.; Takehisa, T.; Fan, S. Effects of Clay Content on the Properties of Nanocomposite Hydrogels Composed of Poly(N-isopropylacrylamide) and Clay. *Macromolecules* **2002**, *35*, 10162−10171.
(32) Haraguchi, K.; Farnworth, R.; Ohbayashi, A.; Takehisa, T. Compositional Effects on Mechanical Properties of Nanocomposite Hydrogels Composed of Poly(N,N-dimethylacrylamide) and Clay. *Macromolecules* **2003**, *36*, 5732−5741.
(33) Kaneko, Y.; Sakai, K.; Kikuchi, A.; Yoshida, R.; Sakurai, Y.; Okano, T. Influence of Freely Mobile Grafted Chain Length on Dynamic Properties of Comb-Type Grafted Poly(N-isopropylacrylamide) Hydrogels. *Macromolecules* **1995**, *28*, 7717−7723.
(34) Zeng, K.; Wang, L.; Zheng, S. Rapid Deswelling and Reswelling Response of Poly(N-isopropylacrylamide) Hydrogels via Formation of Interpenetrating Polymer Networks with Polyhedral Oligomeric Silsesquioxane-Capped Poly(ethylene oxide) Amphiphilic Telechelics. *J. Phys. Chem. B* **2009**, *113*, 11831−11840.
(35) Zheng, Q.; Zheng, S. From Poly(N-isopropylacrylamide)-block-Poly(ethylene oxide)-blockPoly(N-isopropylacrylamide) Triblock Copolymer to Poly(Nisopropylacrylamide)-block-Poly(ethylene oxide) Hydrogels: Synthesis and Rapid Deswelling and Reswelling Behavior of Hydrogels. *J. Polym. Sci., Part A: Polym. Chem.* **2012**, *50*, 1717−1127.
(36) Song, J.; Yu, R.; Wang, L.; Zheng, S.; Li, X. Poly(N-vinylpyrrolidone)-Grafted Poly(N-isopropylacrylamide) Copolymers: Synthesis, Characterization and Rapid Deswelling and Reswelling Behavior of Hydrogels. *Polymer* **2011**, *52*, 2340−2350.
(37) Cong, H.; Li, L.; Zheng, S. Poly(N-isopropylacrylamide)-*block*-Poly(vinyl pyrrolidone) Block Copolymer Networks: Synthesis and Rapid Thermoresponse of Hydrogels. *Polymer* **2013**, *54*, 1370−1380.
(38) Haraguchi, K.; Takehisa, T. Nanocomposite Hydrogels: a Unique Organic-Inorganic Network Structure With Extraordinary Mechanical, Optical, and Swelling/De-swelling Properties. *Adv. Mater.* **2002**, *14*, 1120−1124.
(39) Pound, G.; Aguesse, F.; McLeary, J. B.; Lange, R. F. M.; Klumperman, B. Xanthate-Mediated Copolymerization of Vinyl Monomers for Amphiphilic and Double-Hydrophilic Block Copolymers with Poly(ethylene glycol). *Macromolecules* **2007**, *40*, 8861−8871.
(40) de Gennes, P.-G. *Scaling Concepts in Polymer Physics*; Cornell University Press: Ithaca, NY, 1979.
(41) Dobrynin, A. V.; Rubinstein, M. Theory of Polyelectrolytes in Solutions and at Surfaces. *Prog. Polym. Sci.* **2005**, *30*, 1049−1118.
(42) Vakkalanka, S. K.; Peppas, N. A. Swelling Behavior of Temperature- and pH-Sensitive Block Terpolymers for Drug Delivery. *Polym. Bull.* **1996**, *36*, 221−225.
(43) Vakkalanka, S. K.; Brazel, C. S.; Peppas, N. A. Temperature- and pH-sensitive Terpolymers for Modulated Delivery of Streptokinase. *J. Biomater. Sci., Polym. Ed.* **1997**, *8*, 119−129.
(44) Determan, M. D.; Cox, J. P.; Mallapragada, S. K. Drug Release from pH-Responsive Thermogelling Pentablock Copolymers. *J. Biomed. Mater. Res., Part A* **2007**, *81*, 326−333.
(45) Determan, M. D.; Guo, L.; Lo, C.-T.; Thiyagarajan, P.; Mallapragada, S. K. pH-and Temperature-Dependent Phase Behavior of a PEO-PPO-PEO-Based Pentablock Copolymer in Aqueous Media. *Phys. Rev. E* **2008**, *78*, 021802.
(46) Peleshanko, S.; Anderson, K. D.; Goodman, M.; Determan, M. D.; Mallapragada, S. K.; Tsukruk, V. V. Thermoresponsive Reversible Behavior of Multistimuli Pluronic-Based Pentablock Copolymer at the Air-Water Interface. *Langmuir* **2007**, *23*, 25−30.
(47) Janovák, L.; Varga, J.; Kemény, L.; Dékány, I. Investigation of the Structure and Swelling of Poly (N-Isopropyl-Acrylamide-Acrylamide) and Poly (N-Isopropyl- Acrylamide- Acrylic Acid) Based Copolymer and Composite. *Colloid Polym. Sci.* **2008**, *286*, 1575−1585.
(48) Zhang, J.; Chu, L.-Y.; Li, Y.-K.; Lee, Y. M. Dual Thermo- and pH-Sensitive Poly(*N*-Isopropylacrylamide-Co-Acrylic Acid) Hydrogels with Rapid Response Behaviors. *Polymer* **2007**, *48*, 1718−1728.
(49) Champ, S.; Xue, W.; Huglin, M. B. Concentrating Aqueous Solutions of Water Soluble Polymers by Thermoreversible Swelling of Poly[(N-Isopropylacrylamide)-co-(Acrylic Acid)] Hydrogels. *Macromol. Chem. Phys.* **2000**, *201*, 931−940.
(50) Yoo, M. K.; Seok, W. K.; Sung, Y. K. Characterization of Stimuli-Sensitive Polymers for Biomedical Applications. *Macromol. Symp.* **2004**, *207*, 173−186.
(51) Tian, Q.; Zhao, X.; Tang, X.; Zhang, Y. Hydrophobic Association and Temperature and pH Sensitivity of Hydrophobically Modified Poly(N-isopropylacrylamide/acrylic acid) Gels. *J. Appl. Polym. Sci.* **2003**, *87*, 2406−2413.
(52) Champ, S.; Xue, W.; Huglin, M. B. Thermal Effects in the Synthesis of Thermoresponsive Hydrogels of Poly(N-Isopropylacrylamide-co-Acrylic Acid). *Macromol. Mater. Eng.* **2000**, *282*, 37−43.
(53) Lim, Y. H.; Kim, D.; Lee, D. S. Drug Releasing Characteristics of Thermo- and pH-Sensitive Interpenetrating Polymer Networks Based on Poly(N-isopropylacrylamide). *J. Appl. Polym. Sci.* **1998**, *64*, 2647−2655.
(54) Shin, B. C.; Jhon, M. S.; Lee, H. B.; Yuk, S. H. pH/Temperature Dependent Phase Transition of an Interpenetrating Polymer Network: Anomalous Swelling Behavior above Lower Critical Solution Temperature. *Eur. Polym. J.* **1998**, *34*, 1675−1681.
(55) Adem, E.; Burillo, G.; Bucio, E.; Magaña, C.; Avalos-Borja, M. Characterization of Interpenetrating Networks of Acrylic Acid (Aac) and *N*-isopropylacrylamide (NIPAM) Synthesized by Ionizing Radiation. *Radiat. Phys. Chem.* **2009**, *78*, 549−552.
(56) Burillo, G.; Briones, M.; Adem, E. IPN's of Acrylic Acid and N-isopropylacrylamide by Gamma and Electron Beam Irradiation. *Nucl. Instrum. Methods Phys. Res., Sect. B* **2007**, *265*, 104−108.
(57) Xia, X.; Hu, Z.; Marquez, M. Physically Bonded Nanoparticle Networks: a Novel Drug Delivery System. *J. Controlled Release* **2005**, *103*, 21−30.
(58) Asoh, T.; Kaneko, T.; Matsusaki, M.; Akashi, M. Rapid and Precise Release from Nano-Tracted Poly(N-isopropylacrylamide) Hydrogels Containing Linear Poly(acrylic acid). *Macromol. Biosci.* **2006**, *6*, 959−965.
(59) Asoh, T.; Kaneko, T.; Matsusaki, M.; Akashi, M. Rapid Deswelling of Semi-IPNs with Nanosized Tracts in Response to pH and Temperature. *J. Controlled Release* **2006**, *110*, 387−394.
(60) Kim, S.; Chung, E. H.; Gilbert, M.; Healy, K. E. Synthetic MMP-13 Degradable ECMs based on Poly(N-isopropylacrylamide-co-acrylic acid) Semi-Interpenetrating Polymer Networks. I. Degradation and Cell Migration. *J. Biomed. Mater. Res., Part A* **2005**, *75*, 73−88.
(61) Beltran, S.; Baker, J. P.; Hooper, H. H.; Blanch, H. W.; Prausnitz, J. M. Swelling Equilibria for Weakly Ionizable, Temperature-Sensitive Hydrogels. *Macromolecules* **1991**, *24*, 549−551.
(62) Feil, H.; Bae, Y. H.; Feijan, J.; Kim, S. W. Effect of Comonomer Hydrophilicity and Ionization on the Lower Critical Solution Temperature of N-Isopropylacrylamide Copolymer. *Macromolecules* **1993**, *26*, 2496−2500.
(63) Lee, W.-F.; Yuan, W.-Y. Thermoreversible Hydrogels XI: Effect Of Salt On The Swelling Properties Of The (*N*-Isopropylacrylamide-*Co*-Sodium 2-Acrylamido-2-Methylpropyl Sulfonate) Copolymeric Hydrogels. *J. Appl. Polym. Sci.* **2001**, *79*, 1675−1684.

(64) Kim, J. H.; Lee, S. B.; Kim, S. J.; Lee, Y. M. Rapid Temperature/pH Response of Porous Alginate-*g*-Poly(*N*-isopropylacrylamide) Hydrogels. *Polymer* **2002**, *43*, 7549−7558.
(65) Zarzyka, I.; Pyda, M.; Lorenzo, M. L. D. Influence of Crosslinker and Ionic Comonomer Concentration on Glass Transition and Demixing/Mixing Transition of Copolymers Poly(N-Isopropylacrylamide) and Poly(Sodium Acrylate) Hydrogels. *Colloid Polym. Sci.* **2014**, *292*, 485−492.
(66) Yang, H.; Song, W.; Zhuang, Y.; Deng, X. Synthesis of Strong Electrolyte Temperature-Sensitive Hydrogels by Radiation Polymerization and Application in Protein Separation. *Macromol. Biosci.* **2003**, *3*, 400−403.
(67) Zhang, G.-Q.; Zha, L.-S.; Zhou, M.-H.; Ma, J.-H.; Liang, B.-R. Rapid Deswelling of Sodium Alginate/ Poly(N-isopropylacrylamide) Semi-Interpenetrating Polymer Network Hydrogels in Response to Temperature and pH Changes. *Colloid Polym. Sci.* **2005**, *283*, 431−438.
(68) Patton, D. L.; Mullings, M.; Fulghum, T.; Advincula, R. C. A Facile Synthesis Route to Thiol-functionalized α,ω-Telechelic Polymers via Reversible Addition Fragmentation Chain Transfer Polymerization. *Macromolecules* **2005**, *38*, 8597−8602.